Carrier injection effects on exciton dynamics in GaAs/AlAs resonant-tunneling diodes

A Letters Journal Exploring the Frontiers of Physics

March 2009

EPL, **85** (2009) 67010
doi: 10.1209/0295-5075/85/67010

www.epljournal.org

Carrier injection effects on exciton dynamics in GaAs/AlAs resonant-tunneling diodes

F. J. Teran[1], M. D. Martín[1], J. M. Calleja[1], L. Viña[1], L. Eaves[2] and M. Henini[2]

[1] *Departamento de Física de Materiales and Instituto Nicolás Cabrera, Universidad Autónoma de Madrid 28049 Madrid Spain, EU*
[2] *School of Physics and Astronomy, University of Nottingham - NG7 2RD Nottingham, UK, EU*

received 17 December 2008; accepted in final form 6 March 2009
published online 7 April 2009

PACS 71.35.-y – Excitons and related phenomena
PACS 73.40.Gk – Tunneling
PACS 78.47.Cd – Time resolved luminescence

Abstract – We investigate the dynamics of excitons created in a quantum well embedded in a double-barrier resonant-tunneling diode under applied bias. We find that the exciton dynamics is highly correlated with carrier tunneling processes. The tunneling favors exciton relaxation via exciton-carrier scattering processes.

Introduction. – Resonant tunneling in semiconductor heterostructures has drawn special attention due to its fundamental importance and its relevance in high-speed device applications [1]. The precision available in the design and fabrication of double-barrier resonant-tunneling diodes (DBRTDs) makes possible the study of a wide range of transport phenomena, including tunneling through the discrete electronic energy levels of quantum-confined structures [2]. DBRTDs can be also used to study luminescence excitation mechanisms [3]. They offer, for instance, the possibility of exciton formation when low densities of electrons and holes are simultaneously injected into the quantum well (QW) layer [4,5]. Exciton formation and relaxation processes in QWs are extremely sensitive to the carrier and exciton densities [6–9]. Under non-resonant optical generation conditions, excitons must reduce their K-momentum down to zero in order to recombine and emit a photon. Different scattering mechanisms such as interaction with other excitons, carriers or phonons are involved in the K-relaxation process of excitons and determine their dynamics. In DBRTDs, different aspects related to carrier injection into the QW, such as tunneling rates [10,11], the wave vector value of injected carriers prior to the exciton formation [12], or the applied bias [13], may additionally influence the exciton relaxation and formation processes.

In this letter, we examine the variation of the relaxation dynamics of excitons created in a QW embedded in a DBRTD when electrons and holes are independently injected in the QW layer. This is achieved using a n-i-n DBRTD in which a GaAs QW is formed by two thin AlAs tunnel barriers. When a bias is applied, electrons can tunnel resonantly into the QW from the n-doped GaAs layers located on either side of the barriers. When, under applied bias, the device is illuminated with light whose photon energy is above the GaAs band gap energy, photo-generated holes can also enter the QW. By adjusting the bias and the intensity of the light, we can independently control the number of electrons and holes tunneling in the QW before they form excitons and/or interact with photo-created excitons. Thus, exciton-carrier scattering processes are enhanced under resonant-tunneling conditions and therefore exciton relaxation is favored.

Samples and experimental details. – We measured the current-voltage characteristics, $I(V)$, under illumination conditions, and time-resolved and continuous-wave (cw) luminescence of a n-i-n GaAs/AlAs DBRTD over a wide range of bias. The device was grown by molecular beam epitaxy at 550 °C on a semi-insulating (100) GaAs substrate. It has a symmetric layer sequence, incorporating two 6 nm AlAs barriers and a 9 nm GaAs QW in the undoped intrinsic region. Undoped GaAs spacer layers of 20 nm separate the barriers from n-type doped contact layers with Si doping graded from 2×10^{16} (51 nm thick) through 2×10^{17} (80 nm thick) to $2 \times 10^{18}\,\mathrm{cm}^{-3}$ (100 nm thick). Optical lithography and wet etching were used to process circular mesas of diameter 100, 200, and 400 μm with a metal-free window at the top to provide optical access for luminescence measurements.

Two different excitation wavelengths (λ_{exc}) are employed to photo-generate carriers exclusively in the GaAs spacer layers ($\lambda_{exc} = 805\,\text{nm}$) or in the GaAs spacer layers and in the QW ($\lambda_{exc} = 760\,\text{nm}$). Illumination is generated either by a cw or a pulsed Ti : Al_2O_3 laser, with 2 ps long pulses and a repetition rate of 82 MHz. The luminescence is detected by a CCD and a streak camera for cw and temporal detection, respectively. We fix the illumination power for both λ_{exc}'s under cw and pulsed conditions in order to obtain similar values of current at the R_1 and R_2 bias. In this way, the carrier density in the hole accumulation layer (HAL) is made similar for both λ_{exc}'s, allowing us to compare the effect of different illumination conditions on exciton dynamics.

Experimental results under cw illumination. – Figure 1 shows typical $I(V)$ characteristics of our DBRTD at 4.2 K under cw illumination. In dark conditions, the $I(V)$ curve has a resonance with a peak at $V = +0.195\,\text{V}$, labelled as E_1, which arises from resonant tunneling of conduction band electrons from the electron accumulation layer (EAL) into the lowest energy sub-band E_1 of the QW (see inset of fig. 1a). Under cw illumination, the E_1 resonance slightly shifts towards lower bias by an amount which is sensitive to the illumination power [5]. At the same time, two additional resonances, R_1 and R_2, appear in the $I(V)$ at bias $V_{R_1} = +0.060\,\text{V}$ and $V_{R_2} = +0.105\,\text{V}$, significantly below that of the E_1 resonance peak. Such light-induced resonances have been assigned to resonant tunneling of photo-created holes from the HAL into the HH_1 and LH_1 sub-bands of the QW, respectively [5]. They appear only for photon energies larger than the GaAs band gap and their amplitudes and bias positions strongly depend on the illumination intensity [5].

To understand the effect of illumination we refer to the band profiles of the device shown in the inset of fig. 1a. The incident light creates electron-hole pairs in the depletion region beyond the collector barrier. In forward bias, corresponding to the top n^+ GaAs layer biased positive, the photo-created electrons in the GaAs depletion region beyond the right-hand barrier are swept towards the doped collector region. Hence, photo-created electrons play little role in influencing the optical and electrical properties of the device. In contrast, photo-created holes drift towards the collector barrier where they form a HAL. This process has been discussed previously in the context of photoluminescene (PL) of RTDs [3]. Thus, when $\lambda_{exc} = 805\,\text{nm}$, the QW recombination originates exclusively from tunneling of photo-created holes and electrons from the HAL and the EAL, respectively, leading to an electroluminescence (EL) signal. This recombination process emits photons whose energy has shorter wavelengths ($\sim 795\,\text{nm}$) than λ_{exc}. Such up-conversion processes are assisted by the external bias applied on the device. However, electron-hole pairs are also non-resonantly generated in the QW when $\lambda_{exc} = 760\,\text{nm}$. In this case, the QW emission under applied bias is the sum of PL and EL processes where

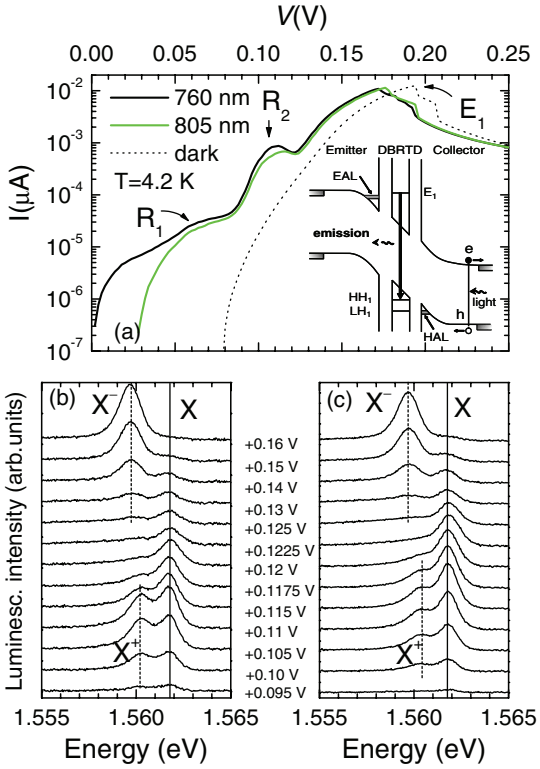

Fig. 1: (Color online) (a) $I(V)$ characteristics at $T = 4.2\,\text{K}$ in forward bias in dark (dotted line) and under *cw illumination* (solid lines) with $\lambda_{exc} = 760\,\text{nm}$ (black) and 805 nm (green) and power 3 and $6\,\text{mW/cm}^2$, respectively. Inset: schematic band diagram showing how the photo-created electron-hole pairs drift in opposite directions under an applied electric field and the recombination process in the QW. (b) Luminescence spectra at different bias under cw illumination with $\lambda_{exc} = 760\,\text{nm}$ and power $3\,\text{mW/cm}^2$. (c) Luminescence spectra at different bias under cw illumination with $\lambda_{exc} = 805\,\text{nm}$ and power $6\,\text{mW/cm}^2$.

the EL emission intensity strongly depends on the applied bias. The space-charge density of the HAL modifies the electrostatic profile in the device by screening the electronic charge in the EAL and in the QW. This accounts for the observed shift to lower bias of the threshold and the peak of the E_1 resonance.

The electrical current flowing through our device can be expressed as $I = n_e A e/\tau$, where e is the electron charge, A is the device area, n_e is the electron density in the QW at a given bias and τ is the time required by an electron to escape from the QW, *i.e.* the electron dwell time, at a given bias. Using the current value at bias E_1 ($I = 10\,\mu\text{A}$), the diameter of the mesa device ($400\,\mu\text{m}$), and $n_e = 1 \times 10^{11}\,\text{cm}^{-2}$ at E_1 bias[1], we obtain $\tau = 20\,\mu\text{s}$ under electron resonant-tunnelling conditions. The cw illumination conditions do not significantly affect the value of τ with respect to dark conditions since the current value at the E_1 resonance bias is roughly the same. The large

[1]The value of n_e was estimated from the magnetoquantum oscillations in the tunnel current of the DBRTD at E_1 bias.

value of τ reflects the long dwell time of electrons in the QW before they tunnel through the collector barrier. This has important consequences for the QW recombination dynamics, as we will discuss later.

The characteristic emission spectra of this device under cw illumination are very sensitive to the density and the polarity of the free carrier charge build-up in the QW, both of which can be tuned by varying the applied bias. As shown in figs. 1b, c the bias dependences of the emission spectra at 4.2 K under cw illumination with $\lambda_{exc} = 760$ nm and 805 nm are similar despite the different illumination powers: 3 and 6 mW/cm^2, respectively. Under such low-illumination conditions, the induced exciton populations in the QW at zero or applied bias $V < +0.090\,V$ are either zero (for $\lambda_{exc} = 805$ nm) or so small (for $\lambda_{exc} = 760$ nm) that no PL is detected. Furthermore, the injection of the photo-created holes entering the QW is so low that the EL signal is also negligible. Only when the applied bias is increased beyond $V > +0.090$ V does the charge environment created inside the QW by the carrier tunneling favor the formation of positive (X^+), neutral (X), and negatively (X^-) charged excitons, leading to a detectable emission for both λ_{exc}. The evolution of the emission spectra with bias is thus highly correlated to hole and electron tunneling, as discussed in detail in ref. [5]. Thus, in the vicinity of V_{R_2} for bias $+0.090\,\mathrm{V} < V < +0.120\,\mathrm{V}$, where holes are the majority carriers in the QW, we can resolve two PL peaks identified as X^+ and X. When the bias is increased away from the hole resonance condition, the X^+ emission decreases with respect to that of X. At bias $V = +0.120$ V, which corresponds to the current valley between R_2 and E_1, only the neutral exciton peak remains visible. A further small increase of bias towards the peak of E_1 gives rise to another well-resolved emission line at lower energy associated with X^- recombination. When the bias $V > +0.130$ V, the electron charging of the QW favors X^- emission (*i.e.* X^- formation), whereas the neutral exciton emission quenches when approaching the E_1 resonance. No quantum-confined Stark effect was observed in the QW emission within the bias range studied.

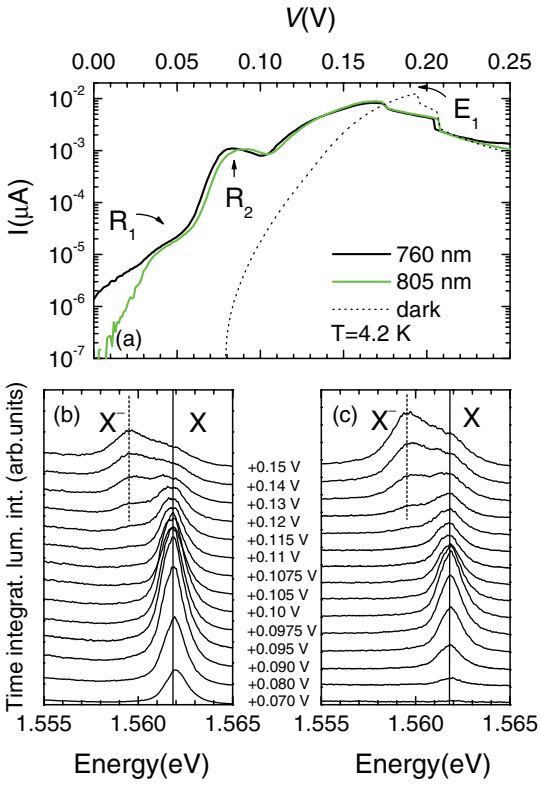

Fig. 2: (Color online) (a) $I(V)$ characteristics at $T = 4.2$ K in forward bias in dark (dotted line) and under *pulsed illumination* (solid lines) with $\lambda_{exc} = 760$ nm (black) and 805 nm (green) and power 120 and 240 mW/cm^2, respectively. (b) Time-integrated luminescence spectra at different bias under pulsed illumination with $\lambda_{exc} = 760$ nm and power 120 mW/cm^2. (c) Time-integrated luminescence spectra at different bias under pulsed illumination with $\lambda_{exc} = 805$ nm and power 240 mW/cm^2.

Experimental results under pulsed illumination. – Under pulsed-illumination conditions, the $I(V)$ curves show similar features to those obtained under cw illumination independently of λ_{exc}, as shown in fig. 2a: light-induced current resonances at $V_{R_1} = +0.040$ V and $V_{R_2} = +0.080$ V and the electron resonance at $E_1 = +0.170$ V. The shifts of the R_1 and R_2 resonances towards lower bias than those observed under cw illumination probably originate from the larger photo-created hole density in the HAL under pulsed conditions, due to the higher power of the laser pulses. In spite of the close resemblance of the $I(V)$ curves, the emission spectra recorded under pulsed excitation reveal substantial differences in the optical transitions with respect to cw experiments. Figures 2b, c show the bias dependence of the time-integrated emission spectra for $\lambda_{exc} = 760$ and 805 nm, respectively. First, there is no trace of X^+ in the emission spectrum in the vicinity of V_{R_2} (*i.e.* $+0.090\,\mathrm{V} < V < +0.11$ V). This is the most remarkable difference in the emission spectra between pulsed and cw illumination conditions. On the other hand, the evolution with bias of the emission spectrum shows a similar behaviour for both λ_{exc}'s. Thus, one can observe X emission within the bias range from $V = 0$ to $V = +0.15$ V, contrary to the cw case where the X line is quenched beyond the minimum between the R_2 and E_1 peaks. Note that the quantum-confined Stark effect is negligible in the whole bias range. The X^- line appears in the vicinity of the E_1 resonance ($+0.11\,\mathrm{V} < V < +0.16$ V), similar to the cw case, but with a weaker emission. At $V = +0.15$ V, the relative emission intensity of the X^- line is comparable to that of the X line, contrary to the cw illumination case, where the X^- line was the only emission. The absence of X^+ emission in the time-resolved spectra suggests that the excess hole density in the QW is too small to form X^+ as compared to the cw case. Similar remarks apply to X^- emission whose time-resolved spectra reflect a weaker relative intensity with respect to X emission which

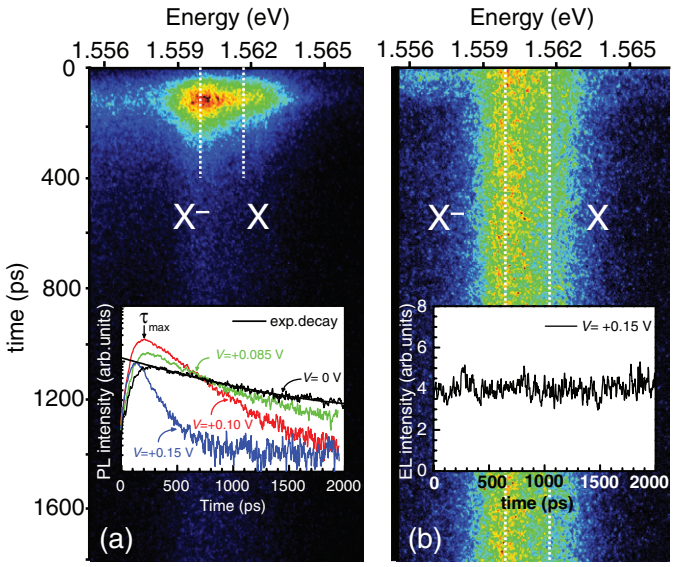

Fig. 3: (Color online) False-colour scale images showing the temporal evolution of X^- and X emissions at $T = 4.2$ K for $V = +0.15$ V under pulsed illumination with: (a) $\lambda_{exc} = 760$ nm and power 120 mW/cm^2. Inset: time evolution traces of the exciton emission intensity at $T = 4.2$ K for different bias. The black thick line is an exponential fit of the decay. The vertical arrow indicates τ_{max}. (b) $\lambda_{exc} = 805$ nm and power 240 mW/cm^2. Inset: Time evolution trace of the exciton emission intensity at $T = 4.2$ K for $V = +0.15$ V bias.

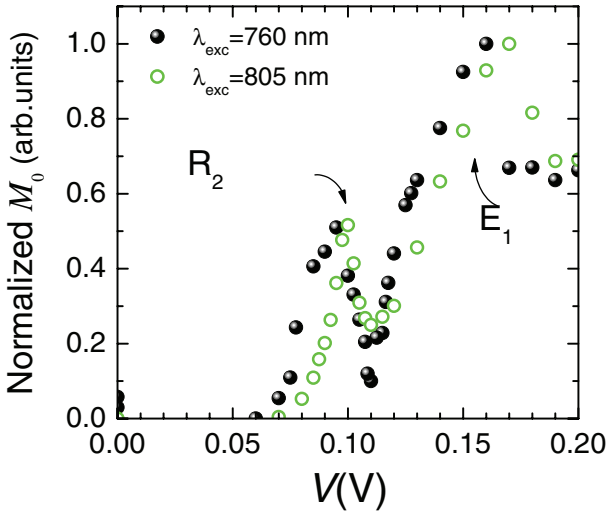

Fig. 4: (Color online) Bias dependence of the normalized M_0 under pulsed illumination with $\lambda_{exc} = 805$ (empty circles) and 760 nm (solid circles) at $T = 4.2$ K.

indicates smaller electron densities inside the QW as compared to the cw case. This can be explained by the extremely slow carrier tunneling rates. Generally, the hole tunneling rate (τ_h^{-1}) is expected to be much smaller than that for electrons [14], which could explain the absence of X^+ emission. This interpretation is also supported by comparing the dynamics of the excitonic emission for the two different λ_{exc}'s at a fixed bias.

Figure 3a, b depicts false-colour scale images representing the temporal evolution of X^- and X recombination at $V = +0.15$ V under pulsed illumination with $\lambda_{exc} = 760$ and 805 nm, respectively. As can be seen, the exciton dynamics depends markedly on λ_{exc}. Whereas for $\lambda_{exc} = 805$ nm, the temporal evolution of the luminescence remains constant in the investigated time range for all bias values, the dynamics is bias dependent and much faster when $\lambda_{exc} = 760$ nm. In the latter case, note that the X^- and X emission decay is similar: the luminescence intensity reaches its maximum after 100 ps and disappears after 350 ps (see fig. 3a). On the other hand, it remains almost constant over the entire temporal span for $\lambda_{exc} = 805$ nm (see fig. 3b). As seen in the inset of fig. 3b, the intensity of the emission at $t = 0$ ps is the same as during the whole time span of our measurements, indicating that the emission at $t = 0$ ps arises from the excitation with the previous pulse, allowing us to establish a lower limit for τ_h, given by the time, t_{rep}, between consecutive pulses of our laser ($\tau_h > t_{rep} = 12$ ns). In the low-bias range studied ($0 < V < +0.22$ V), τ_h is mainly determined by the barrier thickness [13,15]. However, the emission intensity under pulsed excitation significantly varies with the applied bias, as shown in figs. 2b, c.

We have plotted in fig. 4 the normalized time- and energy-integrated emission intensity (zero moment of the emission spectrum, M_0) as a function of bias for $\lambda_{exc} = 760$ nm (solid circles) and $\lambda_{exc} = 805$ nm (empty circles) at $T = 4.2$ K. The bias dependence of the normalized M_0 in the bias range $+0.05\,\text{V} < V < +0.20\,\text{V}$ resembles the $I(V)$ curves independently of λ_{exc}. This reflects a clear correlation of the emission under pulsed illumination with the carrier charging of the QW as in the case of cw illumination [5].

We now consider the case of $\lambda_{exc} = 760$ nm. Under this illumination, there are two contributions to the QW emission: a weak and slow emission signal arising from EL, as described above, for $\lambda_{exc} = 805$ nm and a strong and fast emission signal originating from the recombination of photo-generated carriers in the QW. Thus, the exciton dynamics is dominated by the photo-created X emission and displays a remarkable bias dependence, as depicted in the inset of fig. 3a: an acceleration of the X decay is observed with increasing bias. To gain a further insight into the exciton dynamics, we have extracted the decay time (τ_d) by fitting the decaying part of the temporal traces with an exponential function (see solid line in the inset of fig. 3a). We also extract τ_{max}, which corresponds to the time needed to reach the maximum emission intensity as depicted by a vertical arrow in the inset of fig. 3a.

Figure 5 compares $I(V)$ with τ_d and τ_{max} obtained at different bias. We can clearly observe an overall decrease of τ_d and τ_{max} with increasing bias up to E_1. The τ_d/τ_{max} values vary from 684/245 ps at $V = 0$ V to 149/124 ps at

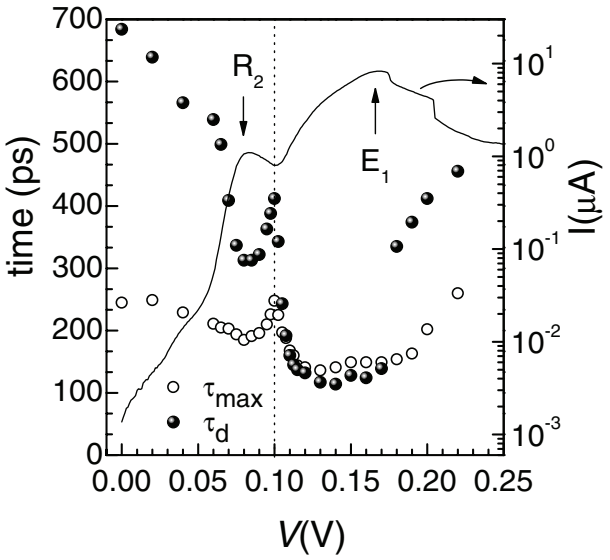

Fig. 5: Comparison of the $I(V)$ characteristic (line) with the bias dependence of τ_{max} (open circles) and τ_d (solid circles) of the X emission at $T = 4.2\,\mathrm{K}$ under pulsed illumination with $\lambda_{exc} = 760\,\mathrm{nm}$ and power $120\,\mathrm{mW/cm^2}$.

$V = +0.160\,\mathrm{V}$. Both times show a similar behaviour with bias: two local minima at R_2 and E_1 and local maxima at the bias valley position of $I(V)$ (dotted line in fig. 5). Such bias dependence reveals clear correlations between τ_d and τ_{max} and between the exciton dynamics and the carrier tunneling processes. Considering that the tunneling times for electrons and holes are several orders of magnitude larger ($> 10\,\mu\mathrm{s}$) than the characteristic exciton dynamics times ($\sim 100\,\mathrm{ps}$), we discard any influence of the carrier tunneling rates on exciton dynamics when $\lambda_{exc} = 760\,\mathrm{nm}$. In order to understand the bias dependence of the exciton dynamics, let us first consider the situation at zero bias. In this case, there are no carriers entering the QW and only photo-created excitons are present in the QW. The energy relaxation of these excitons occurs through X-X and X-phonon scattering mechanisms, leading to a very slow dynamics ($\tau_{max} = 245\,\mathrm{ps}$ and $\tau_d = 684\,\mathrm{ps}$). As the bias is increased, additional charges start to tunnel into the QW (electrons from the EAL and photo-created holes from the HAL), changing the charge environment of the photo-created excitons. The presence of these additional charges in the QW activates the carrier-X scattering processes. These new relaxation mechanisms become evident when approaching the hole resonance bias R_2. Under these conditions, excitons are surrounded by excess holes and scatter with them relaxing their kinetic energy. The hole-X scattering mechanism is more efficient than the X-X scattering process [8], leading to a faster relaxation dynamics and therefore to a reduction of τ_{max} and τ_d. It is worth noting that even though hole tunneling is a very slow process and not many holes enter the QW (no X^+ emission is observed) their density is nevertheless sufficient to modify the exciton relaxation dynamics because the cross-section for the scattering of excitons by holes is one order of magnitude larger than that of scattering by electrons [9]. Any increase/decrease of the applied bias away from R_2 brings the hole tunneling out of resonance. Thus, the number of excess holes inside the QW diminishes and the charge environment evolves back towards neutral conditions.

The effect of X-hole scattering processes is drastically reduced on both sides of R_2 slowing down the exciton relaxation and leading to longer τ_{max} and τ_d. Additionally, the increase of the applied bias that moves the hole tunneling out of resonance simultaneously brings the electron tunneling into resonance, thus steadily augmenting the density of electrons in the QW. Therefore, X^- emission can be observed at $V \geqslant +0.12\,\mathrm{V}$ and X-electron scattering processes accelerate the exciton dynamics, reducing τ_{max} and τ_d when approaching E_1 and obtaining a second local minimum at this bias position. A final bias region, for $V \geqslant +0.18\,\mathrm{V}$, takes the electron tunneling out of resonance leading to: i) a decrease of the free electron density inside the QW, ii) a reduction of X-electron scattering processes and iii) an increase of τ_{max} and τ_d, which slowly return to the values found for neutral-charge environment in the QW.

Conclusions. – We have investigated the exciton relaxation mechanisms in a n-i-n DBRTD. The absence of X^+ emission in the time-resolved spectra suggests that the hole tunneling rate is several orders of magnitude shorter than that of electrons. Furthermore, we have provided evidence that the exciton dynamics is controlled by exciton-carrier scattering mechanisms in DBRTD under carrier resonant-tunneling conditions.

* * *

This work has been partially supported by the Spanish MEC (MAT2008-01555/NAN, and QOIT CSD2006-00019), the CAM (S-0505/ESP-0200), IMDEA-Nanociencia and by EPSRC (UK). MDM acknowledges financial support from the Ramon y Cajal Programme.

REFERENCES

[1] Mizuta H. and Tanoue T., *The Physics and Applications of Resonant Tunnelling Diodes*, edited by Ahmed H., Pepper M. and Broers A., Vol. **2** (Cambridge University Press, Cambridge) 1995, p. 1.

[2] Vdovin E. E., Levin A., Patanè A., Eaves L., Main P. C., Khanin Yu. N., Dubrovskii Yu. V., Henini M. and Hill G., *Science*, **290** (2000) 122.

[3] Skolnick M. S., Simmonds P. E., Hayes D. G., Higgs A. W., Smith G. W., Pitt A. D., Whitehouse C. R., Hutchinson H. J., White C. R. H., Eaves L., Henini M. and Hughes O. H., *Phys. Rev. B*, **42** (1990) 3069.

[4] Buhmann H., Mansouri L., Wang J., Beton P. H., Mori N., Eaves L., Henini M. and Potemski M., *Phys. Rev. B*, **51** (1995) 7969.

[5] Teran F. J., Eaves L., Mansouri L., Buhmann H., Maude D. K., Potemski M., Henini M. and Hill G., *Phys. Rev. B*, **71** (2005) 161309.
[6] Szczytko J., Kappei L., Berney J., Morier-Genoud F., Portella-Oberli M. T. and Deveaud B., *Phys. Rev. Lett.*, **93** (2004) 137401.
[7] Damen T. C., Shah J., Oberli D. Y., Chemla D. S., Cunningham J. E. and Kuo J. M., *Phys. Rev. B*, **42** (1990) 7434.
[8] Honold A., Schultheis L., Kuhl J. and Tu C. W., *Phys. Rev. B*, **40** (1989) 6442.
[9] Feng Y. P. and Spector H. N., *IEEE J. Quantum Electron.*, **24** (1988) 1659.
[10] Van Hoof C., Goovaerts E. and Borghs G., *Phys. Rev. B*, **41** (1992) 6982.
[11] Romandić I., Bouwen A., Goovaerts E., Van Hoof C.and Borghs G, *Semicond. Sci. Technol.*,**15** (2000)664.
[12] Cao H., Klimovitch G., Björk G. and Yamamoto Y., *Phys. Rev. Lett.*, **93** (2004) 137401.
[13] Norris T. B., Song X. J., Schaff W. J., Eastman L., Wicks G. and Mourou G. A., *Appl. Phys. Lett.*, **54** (1989) 60.
[14] Tsuchiya M., Matsusue T. and Sakaki H., *Phys. Rev. Lett.*, **59** (1989) 2356.
[15] Jackson M. K., Johnson M. B., Chow D. H., McGill T. C. and Nieh C. W., *Appl. Phys. Lett.*, **54** (1989) 552.